Maritime Technology and Engineering – Guedes Soares & Santos (Eds)
© 2015 Taylor & Francis Group, London, ISBN 978-1-138-02727-5

Impact resistance of marine sandwich composites

T. Castilho, L.S. Sutherland & C. Guedes Soares
Centre for Marine Technology and Engineering (CENTEC), Instituto Superior Técnico, Universidade de Lisboa, Lisbon, Portugal

ABSTRACT: This work is motivated by the ever increasing range of applications of sandwich composite materials in the marine industry. A brief literature review is presented, followed by the manufacture and flexure, quasi-static and impact tests of a series of marine sandwich composites. Different core materials (PVC, Balsa Corecork NL10 and NL20) are used to produce a sandwich laminate, with E-glass/polyester skins. Drop-weight tests are performed until the failure of the second skin. PVC and NL20 specimens show predictability and repeatability of results, while NL10 present different failure modes and higher absorbed energy. Apart from the peak forces at the failure of both skins, that are around 1.5 times higher in the impact tests, the overall behaviour of the PVC, Balsa and NL20 specimens is well predicted by quasi-static tests. On the other hand, NL10 specimens' behaviour change dramatically from static do impact test, increasing 3 times the absorbed energy. This work indicates that cork sandwich composites have potential in applications with impact requirements, with the downside of lower stiffness and higher weight.

1 INTRODUCTION

Composite materials have been widely used in the marine industry, in an ever increasing range of applications. The concern with the weight of the hull of racing craft led to the construction of sandwich hulls, instead of single skin hulls, and to the use of new materials and methods. A similar trend was observed in some types of military vessels and even in fishing vessels. Sandwich construction allows a panel to have less weight than a single skin panel with the same bending stiffness.

Marine applications tend to require low-cost and low-maintenance solutions, such as GRP. A typical marine sandwich composite would have glass-polyester skins, and would use a relatively cheap core material, as PVC foam. The panels studied in this work use a similar layout as the one used in the European project, MOSAIC, as described in Sutherland et al. (2014), which have already been used in the study of some steel-composite joints (Kotsidis et al. 2014., Kharghani et al. 2014). It consists of a sandwich with 30 [mm] core and 2.5 [mm] facings. It is a layout that is being studied and designed according to the standards.

The application of composites in light-weight and high speed craft, impact resistance properties of the laminates became an even bigger concern. Laminated composite structures are generally more susceptible to impact damage than similar metallic structures. Composite materials have the ability of developing internal damage, almost impossible to be detected, and that can lead to a premature failure of the structure.

There is one innovation introduced in this study which is the consideration of cork as a possible material for the core of the sandwich, which has not been considered in the MOSAIC project, and is not one of the common materials used. It must be recognised that it is not the first time this material is used as the application of cork in high performance sailing craft sandwich structures was studied by Dumont & Blake (2012). Corecell M80 and Corecork NL20 were used to manufacture fiberglass epoxy sandwich panels. The panels were compared in a 3-point bending test and in a drop slamming test. In the bending tests, the panels with cork core are almost equivalent to the PVC ones. The dynamic tests showed a lower rigidity of the cork panels, hence the higher defections of the panels. Also due to the higher weight of the panels, it was concluded that these panels are not suitable for high performance applications.

2 IMPACT ON MARINE COMPOSITES

2.1 *General impact*

First it is important to define the difference between low-velocity impact and high-velocity, or ballistic impact. The low-velocity impacts are those in which stress wave propagation through the thickness of the specimen has no significant importance and can be treated as a quasi-static indentation

(Abrate, 1998). When there is a collision between two bodies, a certain pressure distribution is developed and can be represented by a contact law.

The indentation, α, is defined as the difference in the displacement of the projectile and that of the back face of the laminate. The force between the two bodies with homogeneous and isotropic materials during the indentation process can be described by the Hertzian contact law (Abrate, 1998):

$$P = k\alpha^{\frac{3}{2}} \tag{1}$$

where k is a coefficient that depends on geometry (radius) and material properties of both bodies (Young Modulus, E and Poison's ratio, ν).

To model the dynamics of an impact event, different methodologies can be used, such as spring-mass models, energy considerations through beam theories (Carvalho & Guedes Soares, 1996, Abrate, 2001).

However, due to the complexity of an impact event, it is important to perform experimental testing. Generally, impact testing consists in striking a structure with an indenter or projectile according to a certain mechanism that allows for the calculation of the impact energy and speed.

The fact that composite structures are heterogeneous and anisotropic, leads to a large variety of failure modes. There are four main failure modes regarding single skin laminates: matrix damage, debonding or delamination, fibre breakage and penetration. For sandwich structures, one should consider: face crushing, face shear failure, in-plane failure of faces, flexural failure of faces, core buckling/crushing, core shear failure and core/face debonding (Hildebrand, 1996).

NDE techniques are necessary to analyse the existence, location and extent of internal damage in in-service composite structures. After knowing the location and extent of a certain damage, it is then important to relate the damage with the decrease of the capacity to withstand loads.

2.2 *Impact on marine composites*

Research has been developed in the last years regarding collisions with floaters and other important impact events in high speed craft (Ping et al. 2002). The effect of these loadings can be generally assessed by performing drop-weight tests, with appropriate force, energy and impactor.

Davies et al. (1996) and Choqueuse et al. (1999) developed general experimental research regarding different impact scenarios in marine structures, with the main objective of getting comparative results with the developed predictive methods. Glass reinforced plastic with PVC foam sandwich was submitted to a low energy drop-weight test. The results were reasonably predicted by FEM models.

Johnson et al. (2009) performed FEM models with progressive damage in large simply supported glass woven Vinylester panels, and the results compared with full scale tests.

The use of cheaper quasi-static tests to assess the impact resistance of marine GRP was studied by Sutherland & Guedes Soares, (2012). A good approximation of the initiation of delamination and dynamic force-deflection behaviour at low to medium incident energies was obtained. After a set of impact tests, it was concluded that larger specimens present relatively lower load and displacement at fibre failure, less membrane effects and more irreversibly absorbed energy than smaller specimens.

Davies (1999) studied the effect of scaling in impact testing of GRP-PVC sandwich laminates. Geometrical scaling factor was visible on the experimental results, with better results for the panels where shear is predominant over bending and membrane effects. More results on scaling are reported by Sutherland & Guedes Soares, (2007).

An extensive experimental work regarding single skin composites was performed over the last years by Sutherland & Guedes Soares, (1999, 2004, 2005a, b, 2006). They have concluded that the high performance of a certain materials under impact depends on many parameters, thus the difficulty to standardize impact test and design. Besides material properties and manufacturing techniques, structural configuration has a main importance on the damage failure modes.

Wiese et al. (1998) performed oblique impact tests on a series of sandwich panels, with different thicknesses and cores (PVC foam and balsa). According to these studies, core material has little influence on the impact strength of the outer skin. Balsa core tends to promote more back skin delaminations, while PVC develops more delaminations on the impact skin.

Echtermeyer et al. (1994) conducted a study concerning composite structures for high speed craft. It was concluded that collision with floating objects is more critical than slamming loads. They developed a method for designing lighter hybrid glass-aramid laminates, maintaining the impact strength of pure glass fibre panels.

An extensive literature review on the effects of strain-rate on the impact strength of FRP sandwich skin and core materials was presented by Hildebrand (1997). Typically, the strength of the materials increases with increasing strain rate. The fact that most of material properties for the design of composites are based in quasi-static tests can

induce the choice a material that is not the best for the impact scenario. With the increase of strain rates from quasi-static to impact scenarios, the increase in strength can be up to 40 [%] for glass polyester skins and up to 80 [%] for some low density PVC core foams.

3 EXPERIMENTAL PROCEDURES

3.1 *Specimen preparation*

From the standard ASTM C 393, the test should verify 2 conditions: the ultimate strength of the skins and the core compressive strength must not be exceeded. However, the wide variety of core material mechanical properties used in this work (Table 1) made it impossible to set a length that would comply with the above criteria. It was decided to produce the beams long enough, and then, experiment what would be the bending span, so that the shear failure is visible in all specimens and the results are easily comparable. A width of approximately 70 [mm] was used.

The panels were manufactured using vacuum bagging technique. Amorim Cork Composites provided Corecork NL10 and NL20. Besides the facilities and technical support during manufacturing, the Estaleiros Navais de Peniche provided the remaining core materials, glass reinforcement, resin and catalyst, consumables for vacuum bagging and safety equipment (Table 2).

The panels were built in two stages, one for each skin.

- The core plates were treated with resin dissolved in acetone, to reduce the porosity and increase adhesion.
- The resin was mixed with the catalyst, with an approximate ratio of 20 [mL/Kg].
- On the lamination platform, the 4 layers of reinforcement corresponding to one skin, were laminated with a roller.

Table 1. Relevant mechanical properties of the core materials utilized.

	NL10	NL20	Divinycell H100	Baltek 100
Density [Kg/m³]	120	200	100	153
Shear modulus [MPa]	5.9	5.9	35	309
Shear strength [MPa]	0.9	0.9	1.6	3
Comp. modulus [MPa]	5.1	6	135	4005
Comp. strength [MPa]	0.3	0.5	2	12.9

Table 2. Materials utilized in the manufacture of the sandwich panels.

Material	Quantity
Corecork NL10	2 * 1000 * 500 * 30 [mm]
Corecork NL20	2 * 1000 * 500 * 30 [mm]
Divinycell H100	2 * 1000 * 500 * 30 [mm]
Baltek 100	1 * 1219 * 609 * 31.7 [mm]
E-Glass LT800 E 10[a] 0/90 Biaxial	35 [m] * 1.4 [m]
Resin Crystic 489 PA BT LV	22.40 [Kg]
Catalyst Butanox M-50	424 [mL]

- After lamination of the skin, the core plate was placed on top, followed by the peel ply, breather and vacuum bag.
- The vacuum was applied (–0.8 [bar]) and kept for 6 hours.

This process was repeated for the remaining skin.

During and after the completion of the manufacture of the panels, it was observed that the cork panels absorb more resin than PVC and Balsa. Other phenomena is the fact that the skins present a rather irregular surface, believed to be related with small breaches in the sealant tape and with the use of bidirectional reinforcement as the last layer, instead of a more common CSM layer. In the end, the panels were named with the type of core material (NL10, NL20, PVC and Balsa) followed by a number (1 or 2).

After the manufacture of the panels, they needed to be cut into beams and small plates. After some attempts, the final solution was to use a water refrigerated diamond disk saw, typically used to cut stone and concrete. Due to the water flow on the disk, the dust from the skin and core can be easily removed. The specimens were then let drying for a few days.

The dimensions of each specimen were then measured with a digital calliper. Figure 1 and Figure 2 show the total thickness and the thickness of each skin of each panel, respectively.

There is not much variation on the thickness of the core plates. However, there is some variation on the thickness of the skins. The first and second skin was defined according to the thickness. The outer skin (first skin or skin on the impact side) is typically thicker than the inner skin (second skin). The variability in thickness of the skins is dependent on the amount of resin and pressure applied with the roller on the laminate. The vacuum bag applies pressure against the core, "squeezing" the resin from the skin.

There seems to be a relation between the thickness of the skins and the porosity or capacity to

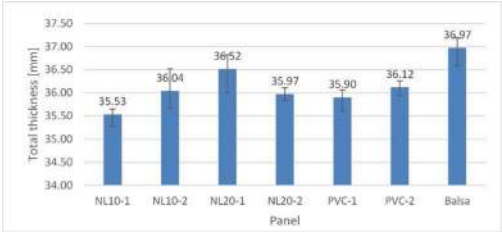

Figure 1. Total thickness of the manufactured panels.

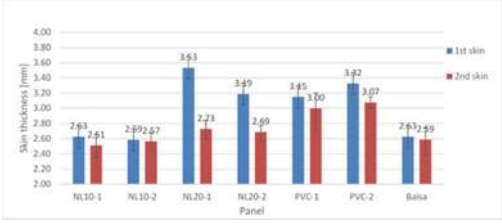

Figure 2. Skin thickness of the manufactured panels.

absorb resin in the core. NL10 and balsa panels are the ones with more porosity and present the smallest thicknesses in the skin. The variation on the thickness from one skin to the other, in the same panel, can also be explained by the capacity to absorb resin. One could say that when producing the second skin, the core has less porosity, since some of the voids are filled with resin, thus leaving more resin on the skin.

Figure 3 presents the average density for each manufactured panel, and two main remarks can be taken from the results. The first is that there is a significant difference in the density of cork panels, PVC and balsa. The second is that even though the density of the NL10 cork is almost half of the NL20, the densities of the panels produced from both cores are almost identical. The same happens with PVC and balsa panels, although in this case, balsa is only 1.5 times denser than the PVC foam. For the cork panels, the NL10 panels absorb more resin than the NL20 ones, increasing the density of the final panel. Comparing the PVC and balsa panels, the densities are similar because the PVC panels have thicker skins than the Balsa ones, which compensates the fact that Balsa core is denser than PVC.

It is also relevant to mention that NL10 panels present a sticky surface and a strong almond smell, indicating that something in the Corecork NL10 interfered with the cure, since all the remaining conditions were similar to all panels manufactured (resin batch, temperature, surface preparation, …).

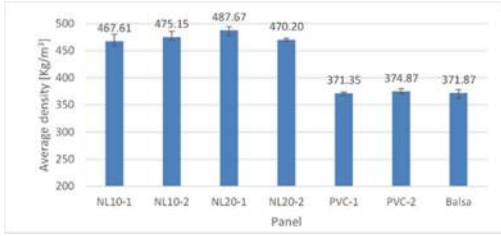

Figure 3. Average density of the manufactured panels.

3.2 *Specimen tests*

In general the tests followed as closely as possible the following standards:

- Core Shear Properties by Beam Flexure (ASTM C 393) (ASTM, 2011)
- Static indentation (ASTM D6264) (ASTM, 1998)
- Impact test (ASTM D 7136) (ASTM, 2005)

Small specimens have been prepared as they were to be tested in an existing hydraulic test machine and a drop-weight machine that are appropriate for that size of specimen. The specimens were used for different types of tests and the reference of each specimen consists in a sequence of the following codes:

- F, S or D—Identifies the type of test: Flexural, Static or Dynamic (impact);
- PVC, NL1, NL2 or BAL—Identifies the core material: Divinycell H100, Corecork NL10, Corecork NL20 or Baltek 100;
- 1 or 2—Number of the panel the specimens were cut from;
- XX—The number of that specimen/test.

3.2.1 *Bending tests*

The wide range of mechanical properties of the core materials used in this work does not comply with the standard ASTM C 393. Hence, the selection of the span and loading pad was also based in some preliminary tests applied to PVC specimens, with constant speeds of 0.2 [mm/s] (Fig. 4).

Although the use of a cylindrical roller removes sharp edges where the failure could start prematurely, it leads to the fact that the load is virtually applied in a line, making the specimen fail prematurely. The use of plates instead of the roller seems to distribute the load evenly. In the test with the 40 [mm] load plate, the specimen withstands more deformation, while shear yield is also better observed, but the use of a large plate under the cylindrical roller induces high instability of the plate.

The span of 280 [mm] with a 20 [mm] plate was then chosen for the remaining tests.

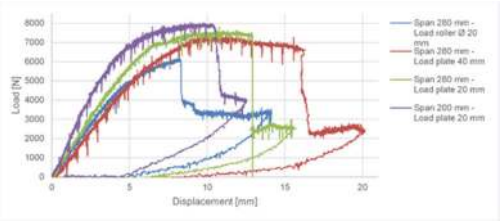

Figure 4. Load vs displacement for different spans and loading pad configurations (unfiltered results).

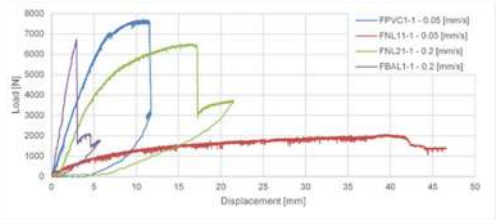

Figure 5. Load vs displacement for first round of tests.

ASTM C393 recommends setting the test speed to produce the failure within 3 to 6 minutes. For PVC test conditions, this corresponds to a speed between 0.07 and 0.03 [mm/s]. The first test, FPVC1-1, was performed with a speed of 0.05 [mm/s].

FNL11-1 was performed with the same speed but the test became too long, because the specimen presents high deflection without breaking.

Figure 5 presents the results for the first round of tests, at different speeds.

To avoid the existing limitations on the data acquisition system, three different speeds were selected for the following 4 rounds tests, depending on core material. FBAL and FPVC tests performed at 0.1 [mm/s], FNL2 at 0.2 [mm/s] and FNL1 at 0.4 [mm/s].

3.2.2 *Quasi-static indentation tests*

Quasi-static tests were performed, using a hemispherical indenter (ø = 16 [mm]), attached to the same load cell, using the same test machine as in the bending tests. The test speed was set to 0.2 [mm/s]. The specimens, with a nominal size of 150 [mm] * 100 [mm] were simply supported on a "picture frame", with the inner dimensions of 100 [mm] * 75 [mm].

First, 2 specimens of each material were tested until complete perforation. Then, 3 specimens of each material were tested until the first failure was noted.

3.2.3 *Impact tests*

Finally, the impact tests were performed, using a Rosand IFW5 falling-weight machine. The machine is connected to a computer, were the position of the weight and the data acquisition process is controlled. Due to friction, the actual speed is accurately measured before impact. The data points consist in a "force" value, which is then converted into speed, displacement and absorbed energy. For the impact tests, the specimens were of the same size as the ones tested under static indentation (150 [mm] × 100 [mm]), and using the same simply supported configuration.

From the absorbed energies in the quasi-static indentation tests, it was decided that the first set of tests would be performed with an energy range between 50 [J] and 200 [J]. For this, a small impact head with a mass of 10.853 [Kg] was used. After performing 2 or more tests for each energy step, it was noted that none of the specimens had suffered penetration of the second skin. With the remaining specimens, additional tests were performed until the failure of the second skin was reached, with the use of a heavier impact head, with 24.269 [Kg].

4 ANALYSIS OF RESULTS

4.1 *Bending tests*

Figure 6 shows the typical behaviour of the beams made of each one of the core materials. In case of the specimen FNL11-2, as for all the NL10 specimens, there was no core failure or skin sudden failure and the tests were stopped at around 35–40 [mm] deflection.

PVC specimens present an almost linear relation between load and displacement, until it reaches a small drop in load, believed to be the shear yield. The force keeps raising at a much lower rate, until the first skin fails, through the combined action of compressive stress in the skin and the out of plane force applied by the load pad.

NL20 specimens present a load-displacement curve similar to PVC specimens, with some differences. The stiffness decreases almost from the beginning and there is no visible shear yield. The specimen fails when a crack appears in the core.

The behaviour of NL10 specimens is rather unexpected, especially because the material properties for Corecork NL10 and NL20 are very similar. These specimens present a very low stiffness and can suffer high deflection without any significant damage. The bad cure of the skins made them more plastic than the skins in the other specimens.

Balsa specimens withstand higher forces than the other specimens, but they fail prematurely (around 3–4 [mm] deflection). The failure occurs at around half the expected core shear strength,

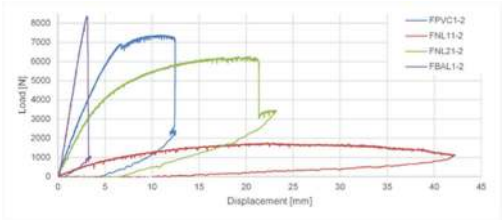

Figure 6. Overview of the typical behaviour for each core material.

and it consists in a core crack, aligned with the core discontinuities, followed by large skin-core debonding.

To help analysing the shear in the specimens, 2% offset curves were calculated, according to ASTM C 393. For the test span of 280 [mm], 2% shear strain corresponds to a deflection of 2.8 [mm], assuming pure shear. Yield and offset shear strength are presented in Table 3. In PVC specimens, shear failure occurs before the 2% offset shear.

Comparing the results with the manufacturer information, one can conclude that Balsa and NL10 have a poor performance. In case of NL10, it is not known a certain reason that can explain such a difference. Maybe the compression of the core under the loading pad is related with this phenomenon. Once the first and second skins are no longer parallel, their effectiveness in carrying axial loads drops.

The fact that the manufactured properties for shear are obtained using a different standard test may also influence the results. ASTM C273 tests sandwich or core specimens in a configuration similar to pure shear. That is the expected reason why Balsa specimens fail at half the expected shear strength. Balsa core panels are built with small rectangular pieces of balsa, glued together. When testing a beam, there will inevitably exists some discontinuities in the core, along the beam's length. These discontinuities are a week point, and will induce shear failure.

This shows that the conditions of the laboratory tests may not occur in "real life" applications, and may induce the designer to select the wrong material.

4.2 *Quasi-static indentation*

To analyse the quasi-static test results, the absorbed energy during the specimen indentation was calculated. Figure 7 presents the absorbed energy for PVC specimens.

Table 4 presents the absorbed energies at the failure of first and second skin, as well as the absorbed energy at 57 [mm] displacement.

Both PVC specimens present a similar behaviour. There are two force peaks, one on each skin. Between these two peaks, the force due to friction and core crushing is relatively low.

NL10 presents high deflection of the first skin, prior to skin failure. The skin then goes back to a shape close to the initial one. In one of the tests (SNL11-1), the first drop in the load corresponds to the appearance of a crack on the skin, similarly to what happens in some of the impact test with this core material.

Both NL20 and Balsa present high friction force between the two skins' peaks, and the second skin tend to separate from the core. NL20 specimens present higher force in the second skin penetration, thus making these specimens the ones which absorb more energy.

PVC and NL10 specimens present a good adhesion between skins and core. NL20 specimens present a lower adhesion compared to NL10. However this fact may be biased by the fact that NL10 panels did not reach the same level of cure as NL20. The fact that NL10 skins are less rigid and brittle than NL20 and that NL10 panels seem to have absorbed more resin may result in a lower adhesion of skin and core in the NL20 specimens.

Regarding Balsa specimens, they present the lower adhesion between skin and core of all specimens. The second skin is easily ripped off from the core material.

4.3 *Impact tests*

4.3.1 *Evolution of failure with increasing energy*

PVC specimens present a reproducible and predictable behaviour. Figure 8 presents a sequence of plots of load vs displacement for each one of the nominal incident energies. One can state that the stiffness of the specimen and the maximum force during the impact of first skin do not vary with rising incident energy, and therefore, do not vary with incident speed as well.

After the rupture of the first skin, the force drops and is maintained relatively low until the indenter approached the second skin. The force rises again, although with lower stiffness, due to the densification of the core and start of the deformation of the second skin. As the energy increases, second skin delaminations start to appear. With an energy of 300 [J], the second skin is pierced and some transverse fibre bundles are ripped off during this.

NL10 specimens presented a far less predictable behaviour than PVC specimens. Figure 9 presents one or two load plots for each energy range, depending on the failure mode observed in each energy level.

Unlike the specimens made from the other materials, NL10 specimens present a variation

Table 3. Experimental vs manufacturer shear strength (average).

	Load-disp. slope (N/mm)	Max. force—Offset (N)	Max force—Yield (N)	Shear strength—Offset (MPa)	Shear strength—Yield (MPa)	Shear strength—Manuf. (MPa)
FPVC	1285	7197	6913	1.53	1.47	1.60
FNL1	204	1229	–	0.26	–	0.90
FNL2	1006	5125	–	1.07	–	0.90
FBAL	2656	–	7601	–	1.50	3.00

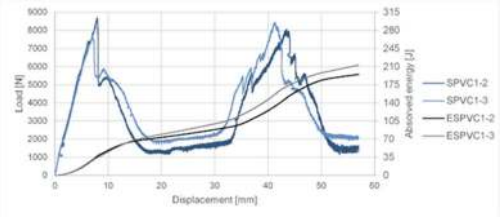

Figure 7. Absorbed energy vs displacement for quasi-static tests on PVC specimens.

Table 4. Absorbed energy at different instants during indentation test (average).

	1st peak			2nd peak		
	Disp. (mm)	Force (N)	Energy (J)	Disp. (mm)	Force (N)	Energy (J)
FPVC	7.51	8103	32.98	42.41	8160	153.36
FNL1	17.77	5398	57.27	41.96	5117	122.26
FNL2	8.07	7654	36.68	44.55	9194	212.76
FBAL	4.46	8688	19.24	44.72	6161	162.81

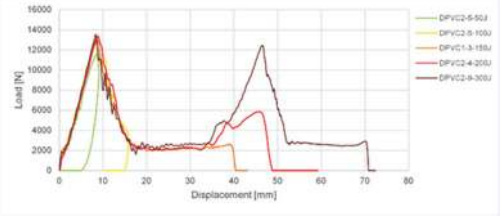

Figure 8. Load vs displacement for impact tests on PVC specimens—50 J–300 J energy range.

on the initial stiffness, prior to the failure of the skin, as well as a wide range of maximum load at which the first failure of the skin occurs. With the amount of data acquired and the variation of both skin thickness and initial velocity, it is impossible to establish any relation between these two properties and the initial stiffness of the specimens.

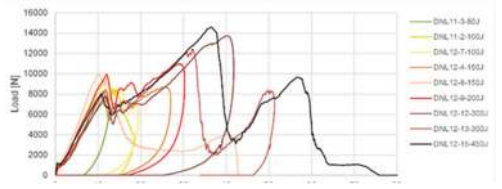

Figure 9. Load vs Displacement for impact tests on NL10 specimens—50–450 J energy range.

A small number of NL10 specimens behave similarly to PVC and NL20 specimens. The first skin is perforated without the appearing of skin cracks, followed by a drop in the load, as the indenter pierced through the core material.

However, the majority of the specimens, the first failure of the first skin is characterized by a transverse crack, with a consequent drop in the load. After, the first failure, the specimen keeps an "elastic" behaviour. For example, some NL10 specimens can withstand a 200 [J] impact without completely penetrating the first skin. At 300 [J], the first skin in one of the specimens is pierced, followed by a sudden drop in the load (DNL12-13). Other specimen does not reach the complete perforation of the first skin, but developed severe shear cracks near the first skin

Only with an incident energy of 450 [J] the specimens are completely perforated. All specimens showed a good adhesion between core and skins, with the appearing of delaminations in the middle of the skin instead of skin/core delamination.

NL20 specimens' initial behaviour is very similar to PVC specimens'. The load increases linearly until the rupture of the first skin, which occurs at around 10 [mm] displacement, between 12,000 and 13,000 [N]. The failure of the first skin consists in perforation of the skin, with some delaminations around the centre.

The load then drops down to around 3000 [N], being the NL20 specimens the ones with higher energy absorption rate in the penetration of the core material.

As the indenter approached the second skin, compressing the cork, the load increases. During

the development of this work, it was observed that cork has the ability to almost completely return to its original shape after compression, similarly to a piece of rubber or a spring. That does not happen with PVC and Balsa. Although these two materials are stiffer than cork, their cells will eventually collapse before cork. Balsa collapses at 0.3% strain and PVC at 1.5%, while NL10 fails at around 5.8% and NL20 at 8.3%, according to Table 1.

The fact that NL20 withstands larger strains before failing may explain the second skin failure mode present in the 300 [J] tests. In these specimens, the second skin completely separated from the specimen. Aligned with the indenter, there is a piece of core material attached to the skin. Bellow that piece of core material, the skin was delaminated and developed cracks.

As the main failure of the second skin corresponds to the delamination of the skin from the core material, and the specimens have relatively small dimensions, it is not possible to state anything about the extent of the delamination in a real life application. However, one can state that if the second skin was not perforated in a specimen this small it will most certainly not be perforated in a larger panel, where bending behaviour dominates.

Similarly to the bending test results, Balsa specimens present higher stiffness than the other composites for impact tests. The maximum force observed in the failure of the first skin is similar to the one verified in PVC and NL20 specimens, and slightly below the maximum force measured in NL10 tests.

After the penetration of the first skin, the load reduces linearly, identically as in the PVC specimens. Then, a plateau between 2000 and 3000 [N] is maintained along almost the complete thickness of the core. At around 40 [mm] displacement, the load starts to increase, for incident energies above 200 [J]. Between the 200 [J] and 300 [J] there is a well-defined difference in the stiffness, when reaching the second skin. For the 300 [J], massive pyramidal cracks were formed in the core material. Still, the difference in the response of the 200 [J] and 300 [J] Balsa specimens second skin occurs at around 40 [mm], suggesting that this difference is not related with the core itself, but with the way the second skin fails. In the tests with 200 [J], the skin did not completely separated from the core, as it happened in the 300 [J] tests.

4.3.2 *Quasi-static testing vs Impact testing*

Once both static and dynamic tests were performed, it would be beneficial to find relations between both results, even if only in a qualitative basis. Among the information that can be obtained from the quasi-static and impact tests is the energy that the specimen can withstand up to the occurrence of a certain failure. The natural choice is to measure the energy absorbed up to the failure of each skin, an important stage in the integrity of the specimens and panels.

The absorbed energy at the displacement where the load reaches a maximum was taken as the absorbed energy up to the failure of first or second skin, respectively.

On the impact tests, the average of the energies for the peaks after and before the failure was considered. They correspond to 200 [J] and 300 [J] for PVC, NL10 and Balsa, and to 300 [J] and 450 [J] for NL10. Figure 12 and Figure 13 present the average absorbed energies for quasi-static and impact tests, respectively. It is noticeable an increase in absorbed energy from the quasi-static tests for the impact tests, especially for NL10 specimens.

Quasi-static data was plotted together with impact data, from Figure 14 to Figure 17. After

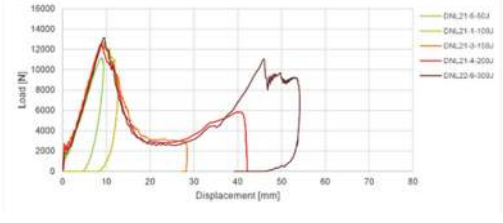

Figure 10. Load vs displacement for impact tests on NL20 specimens—50 J–300 J energy range.

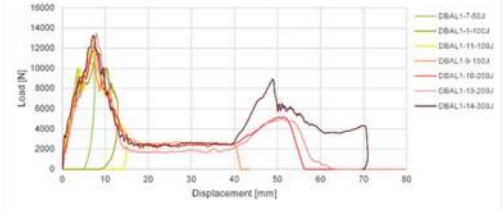

Figure 11. Load vs displacement for impact tests on Balsa specimens—50 J–300 J energy range.

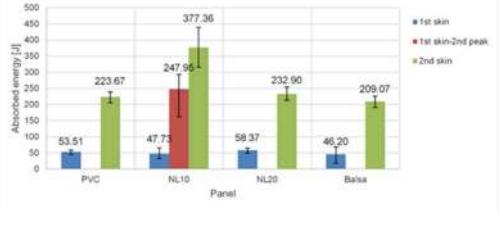

Figure 12. Absorbed energy to reach failure of specimen skins—Quasi-static tests.

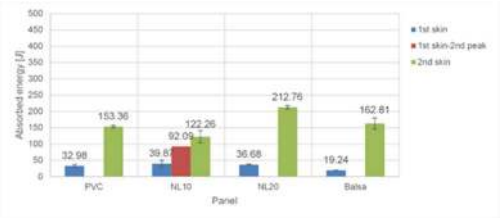

Figure 13. Absorbed energy to reach failure of specimen skins—impact tests.

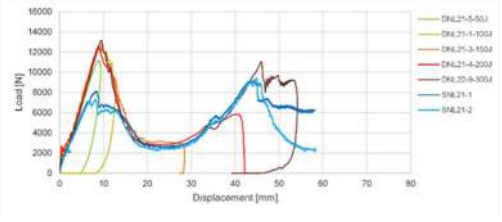

Figure 14. Load vs displacement for NL20 specimens—quasi-static and impact.

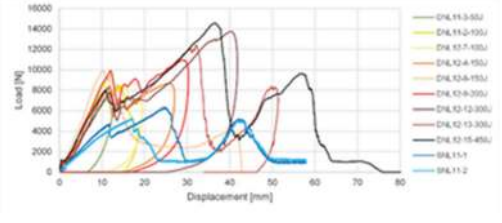

Figure 15. Load vs displacement for NL10 specimens—quasi-static and impact.

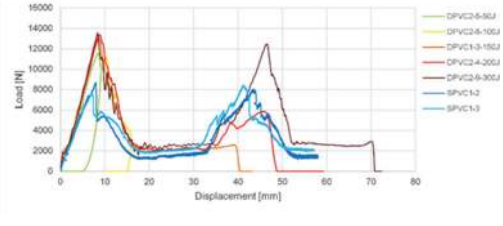

Figure 16. Load vs displacement for PVC specimens—quasi-static and impact.

a brief analysis, one can see that quasi-static tests present a maximum load for the first skin of roughly 2/3 of the maximum impact load.

NL20 seems to present the best results, when comparing quasi-static to impact data (Fig. 14).

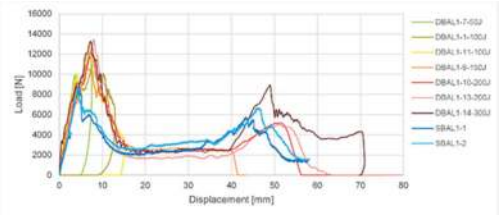

Figure 17. Load vs displacement for Balsa specimens—quasi-static and impact.

Apart from the fact that the maximum load for the first skin is around 2/3 of the one for impact tests, loading and unloading stiffness are very similar.

As stated in the previous section, NL20 specimens present high friction on the core material, which matches quite well the friction from impact tests.

In contrast to NL20 results, NL10 present a large deviation between quasi-static and impact results (Fig. 15). Quasi-static maximum loads are around half the impact maximum loads and the displacements at which the failures of first and second skin occur are also lower. There is also a significant difference between the initial stiffness of the quasi-static and impact results. Additional tests with incident velocities between 0 and 3 [m/s] would help to find a trend line in the highly dynamic behaviour of NL10 specimens. The higher deformations and lower stiffness of the NL10 are related with the bad cure of the skins. This allows the specimen to absorb more energy, similarly to what happens with composites where plasticizers were added to the resin, with the downside of lower stiffness of the panel, which may be a limitation for the application of these panels in structures with high static loads.

Figure 16 and Figure 17 present the comparison of results for PVC and Balsa. Much of the comparison made for NL20 results is applicable for these materials too. The main difference is that the friction force when penetrating the core are not so well defined in PVC and Balsa.

It was previously mentioned in this section that there was a significant increase in the absorbed energy from quasi-static to impact tests, without however doing any reference to the initial velocity. Absorbed energy up to first skin failure increases with incident velocity, for all materials, although more significantly in Balsa specimens.

The increase in the absorbed energy is mainly related with the increase in the maximum force, rather than with the increase in displacement at which first skin failure occurs.

The influence of speed in the maximum force appears to higher between 0 and 4 [m/s], stabilizing for higher speeds. These relations should be further

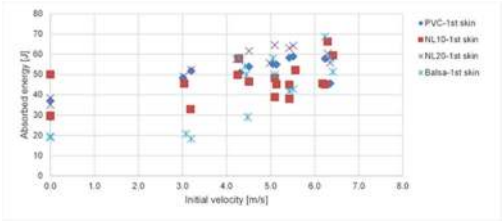

Figure 18. Absorbed energy at failure of first skin vs initial velocity.

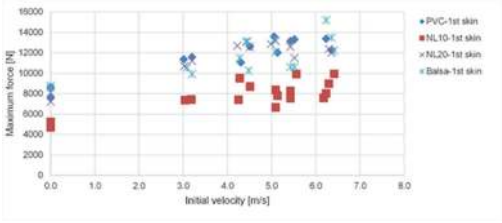

Figure 19. Maximum force at failure of first skin vs initial velocity.

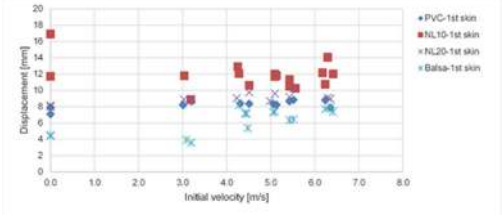

Figure 20. Displacement at failure of first skin vs initial velocity.

investigated through the test of more specimens, and including incident energies between 0 and 3 [m/s] as well.

5 CONCLUSIONS

This reports a test program to compare marine laminates in terms of impact resistance and behaviour.

Four different sandwich laminates were produced, consisting of different core materials (PVC, Balsa, Corecork NL10 and Corecork NL20).

The initial set of bending tests show that the different laminates present a wide range of properties and failure modes. Balsa beams present the higher stiffness but fail at a very low deflection, while NL10 beams withstand large deflections due to the incomplete cure of the skins.

From the static indentation tests, the main considerations are that all four types of specimens present the high forces when the skins are penetrated, with relatively low friction force in the core.

In the impact tests, the criteria to consider a specimen's failure was the penetration or complete separation of the second skin, whichever happened first. However, the separation of the second skin from the core may not be critical in a large panel. The first conclusion from these tests is that NL10 specimens fail between 300 and 450 [J], while the other specimens fail before, between 200 and 300 [J].

PVC and NL20 specimens present a good repeatability of the load-displacement behaviour and of the failure modes, while NL10 specimens present two major failure modes and a far less predictable behaviour. Balsa specimens show a reasonable repeatability of results up to the start of failure of the second skin. After that, the variation in the final behaviour may be explained by the weak skin-core bond.

In the final stage of the work, impact and quasi-static results were compared. PVC, NL20 and Balsa present similar behaviour in static and impact tests, but with the maximum forces around 1.5 times higher for impact tests. The absorbed energy at the failure of first and second skin is then slightly higher in the impact tests. On the other hand, NL10 specimens present a large difference between the two tests. While in the quasi-static tests, NL10 are the specimens which absorb less energy up to the failure of second skin, in the impact tests they absorb substantially more than the other specimens, and 3 times more than the NL10 in quasi-static tests. This behaviour is related with the high deformations allowed by the low stiffness and higher plasticity of the skins.

Finally, one can conclude that cork laminates have potential for applications with impact requirements, with the downside of lower stiffness and higher weight.

REFERENCES

Abrate, S. (1998). *Impact on composite structures*. Cambridge University Press.

Abrate, S. (2001). Modeling of impacts on composite structures., Compos. Struct., vol. 51, pp. 129–138.

Carvalho, A., & Guedes Soares, C. (1996); Dynamic Response of Rectangular Plates of Composite Materials Subjected to Impact Loads. Composite Structures. 34:55–63.

Choqueuse, D., Baizeau, R., & Davies, P. (1999). Experimental studies of Impact on Marine Composites. *Proceedings ICCM12*, Paper 193. Paris.

Davies, G.A.O., Hitchings, D., & Zhou, G. (1996). Impact damage and residual strengths of woven fabric glass/polyester laminates. *Composites Part A:* 1147–1156.

Davies, P. (1999). Scale and size effects in the mechanical characterization of composite and sandwich materials. *ICCM12 Paper 1033*.

Dumont, A.M., & Blake, S.J.I.R. (2012). Application of novel cork sandwich core for high performance sailing craft. Msc Thesis. University of Southampton.

Echtermeyer, A., Pinzelli, R.F., Raybould, K.B., & Skomedal, N. (1994). Advanced composite hull structures for high speed craft. *Proceedings of the 15th International Conferance and Exhibition of the Society for the Advancement of Materials and Process Engineering* (SAMPE). Toulouse.

Hildebrand, M. (1996). A comparison of FRP-sandwich penetrating impact test methods. *Publication 281* VTT Technical Research Centre of Finland Espoo.

Hildebrand, M. (1997). The effect of the strain rate on the strength of FRF-sandwich face and core materials. *Publication 317*. VTT Technical Research Centre of Finland Espoo.

Johnson, H.E., Louca, L. a., Mouring, S., & Fallah, a. S. (2009). Modelling impact damage in marine composite panels. *International Journal of Impact Engineering*, *36*(1), 25–39.

Kharghani, N., Guedes Soares C., & Milat, A. 2014, Analysis of the stress distribution in a composite to steel joint, Guedes Soares, C. & Santos T.A., (Eds.) *Maritime Technology and Engineering* London, UK: Taylor & Francis Group.

Kotsidis, E.A. Kouloukouras I.G. & Tsouvalis, N.G. 2014, Finite element parametric study of a composite-to-steel-joint, Guedes Soares, C. & Santos T.A., (Eds.) *Maritime Technology and Engineering* London, UK: Taylor & Francis Group.

Ping, Y., Weihua, L., & Hayman, B. (2002). Recent Research of High Speed Vessels in Structural Response to Accidental loads. *Journal of Wuhan University of Technology*, *26*.

Standard Test Method for Core Shear Properties of Sandwich Constructions by Beam Flexure. (2011). ASTM.

Standard test method for measuring the damage resistance of a fiber-reinforced polymer matrix composite to a drop-weight impact event. (2005). ASTM.

Standard test method for measuring the damage resistance of a fiber-reinforced polymer-matrix composite to a concentrated quasi-static indentation force. (1998). ASTM.

Sutherland, L.S. and Guedes Soares, C. (1999), Effects of Laminate Thickness and Reinforcement Type on the Impact Behaviour of E-Glass/Polyester Laminates. Composites Science and Technology. 59:2243–2260.

Sutherland, L.S. and Guedes Soares, C. (2004), Effect of Laminate Thickness and of Matrix Resin on the Impact of Low Fibre-Volume, Woven Roving E-Glass Composites. Composites Science and Technology. 64:1691–1700.

Sutherland, L.S. and Guedes Soares, C. (2005a), Contact Indentation of Marine Composites. Composite Structures. 70(3):287–294.

Sutherland, L.S. and Guedes Soares, C. (2005b) Impact Characterisation of Low Fibre-Volume Glass Reinforced Polyester Circular Laminated Plates. International Journal of Impact Engineering. 31(1):1–23.

Sutherland, L.S. & Guedes Soares, C. (2006). Impact behaviour of typical marine composite laminates. *Composites Part B Engineering*, 37(2–3), 89–100.

Sutherland, L.S., & Guedes Soares, C., (2007). Scaling of Impact on Low Fibre-Volume Glass-Polyester Laminates. Composites Part A. 38:307–317.

Sutherland, L.S., & Guedes Soares, C. (2012). The use of quasi-static testing to obtain the low-velocity impact damage resistance of marine GRP laminates. *Composites Part B*, 43(3), 1459–1467.

Sutherland, L.S. Alizadeh F. & Guedes Soares C., 2014, Flex-ural testing of sandwich laminates for steel-composite joints Guedes Soares, C. & Santos T.A., (Eds.) Maritime Technology and Engineering London, UK: Taylor & Francis Group.

Wiese, M., Echtermeyer, A., & Hayman, B. (1998). Evaluation of oblique impact damage on sandwich panels with PVC and balsa core materials. *Fourth International Conference on Sandwich Construction*, *2*, 807–818.